

# Spherical Mapping and Analysis of Aircraft Angles for Maneuvering Flight

Juri Kalviste\*

Northrop Corporation, Hawthorne, California

A spherical mapping technique has been developed for displaying attitude angles of aircraft and flight path in three-dimensional maneuvering flight. The three sets of aircraft angles are the Euler angles, flight path angles, and aerodynamic angles. A computer graphics display has been developed. The display shows the interrelationship among these angles. The aircraft and velocity vector axes of rotation are also shown by the same mapping. Using this display, it is clearly shown that for a coordinated maneuver, the aircraft does not roll about the velocity vector. A coordinated maneuver is achieved by rolling the aircraft about the axis of rotation of the velocity vector. The spherical mapping is also used to derive useful relationships among the aircraft angles.

## Nomenclature

$g$	= acceleration due to gravity, $\text{ft/s}^2$
$n_x$	= load factor along body $x$ axis, $g$
$n_y$	= load factor along body $y$ axis, $g$
$n_z$	= load factor along body negative $z$ axis, $g$
$P, Q, R$	= aircraft rotation vector resolved about body $x$ , $y$ , and $z$ axes, respectively
$U, V, W$	= aircraft velocity vector resolved about body $x$ , $y$ , and $z$ axes, respectively, $\text{ft/s}$
$V_T$	= total velocity $(U^2 + V^2 + W^2)^{1/2}$ , $\text{ft/s}$
$X, Y, H$	= aircraft and target position coordinates ( $X, Y$ ) horizontal, ( $H$ ) vertical positive up
$\Psi$	= aircraft heading angle, horizontal angle between some reference direction (e.g., north) and the projection of the aircraft $x$ axis on the horizontal plane; positive rotation is from north to east
$\theta$	= aircraft pitch angle, vertical angle between the aircraft $x$ axis and the horizontal plane; positive rotation is up
$\Phi$	= aircraft roll angle, the angle between the aircraft $x$ - $z$ plane and the vertical plane containing the aircraft $x$ axis; positive rotation is clockwise, about the $x$ axis, looking forward
$\sigma$	= flight path heading angle, horizontal angle between some reference direction (e.g., north) and the projection of the velocity vector on the horizontal plane; positive rotation is from north to east
$\gamma$	= flight path elevation angle, vertical angle between the velocity vector and the horizontal plane; positive rotation is up
$\mu$	= flight path bank angle, the angle between the plane formed by the velocity vector and the lift vector, and the vertical plane containing the velocity vector; positive rotation is clockwise, about the velocity vector, looking forward
$\alpha$	= angle of attack, the angle between the aircraft $x$ axis and the projection of the velocity vector on the aircraft $x$ - $z$ plane; positive rotation is from the $z$ axis toward the $x$ axis

Presented as Paper 86-2283 at the AIAA Atmospheric Flight Mechanics Conference, Williamsburg, VA, Aug. 18-20, 1986; received June 22, 1986; revision received Oct. 21, 1986. Copyright © American Institute of Aeronautics and Astronautics, Inc., 1986. All rights reserved.

\*Senior Technical Specialist, Control Systems Research, Aircraft Division. Associate Fellow AIAA.

$\beta$	= sideslip angle, the angle between the velocity vector and the aircraft $x$ - $z$ plane; positive direction is when the velocity vector is to the right of the $x$ - $z$ plane, when looking forward
$\tau$	= total aerodynamic angle, $\cos^{-1}(\cos\alpha \cos\beta)$
$\omega$	= total aircraft rotation vector $(P^2 + Q^2 + R^2)^{1/2}$
$\omega_{PR}$	= aircraft rotation vector component in the $x$ - $z$ plane $(P^2 + R^2)^{1/2}$

## Subscripts

$B$	= body axis
$E$	= Earth axis
$p$	= pipper
$PR$	= aircraft rotation vector component in the $x$ - $z$ plane
$R$	= aircraft axis of rotation in body coordinates
$S$	= stability axis
$T$	= target
$v$	= velocity vector axis of rotation in body coordinates
$vw$	= velocity vector axis of rotation in wind axes
$W$	= wind axis

## Superscripts

$(\cdot)$	= derivative with respect to time
$(\cdot)'$	= azimuth and elevation angle of vector projection in $x$ - $z$ plane

## Introduction

In order to analyze aircraft maneuvers, the engineer must know the aircraft attitude, flight path direction, and aircraft attitude relative to the flight path. In particular, to analyze the control of aircraft rolling motion, the engineer must also know the direction of the aircraft axis of rotation in inertial coordinates and relative to the direction of flight. The relative attitude of the aircraft and flight path is defined by angles between the aircraft coordinates, inertial coordinates, and flight path (velocity) vector. Conventionally, we plot each of these angles, representing three-dimensional motion, as a function of time for a given maneuver. However, these time history plots do not clearly show the interrelationship among the angles.

For some simple restricted maneuvers, we can show the angular relationships on a two-dimensional plot. If we consider only the longitudinal motion of the aircraft in the vertical plane, with zero sideslip angle and roll angle, the angular relationship can be represented as shown in Fig. 1. For the directional motion of the aircraft in the horizontal plane, with the

pitch angle, angle of attack, and roll angle being zero, the angular relationship can be represented as shown in Fig. 2. These two two-dimensional representations of angles apply only under the restricted condition where all the angles are defined in the same plane. For more general maneuvering conditions, these relationships do not apply. Unfortunately, these simple relationships are sometimes used under conditions where they do not apply, since these are the only simple relationships that can easily be visualized.

The more general definition of the angular relationships involves angles between vectors in three dimensions. The three-dimensional relationship is then represented by a two-dimensional figure. A typical example of such definitions of the angles is shown in Fig. 3.<sup>1</sup> Two sets of angles are defined. One set consists of the Euler angles  $(\Psi, \theta, \phi)$ , which relate the aircraft attitude to inertial coordinates. The other set consists of the aerodynamic angles  $(\alpha, \beta)$ , which relate the velocity vector to the aircraft coordinates. A third set, which consists of the flight path angles  $(\sigma, \gamma, \mu)$  is not shown, since this would make the figure overly complicated. Another reason for omitting the flight path angle set from this figure is that this set of angles is redundant. For example, in Fig. 1 the orientation of the aircraft  $x$  axis and velocity vector can be defined by the two angles  $\theta$  and  $\alpha$ . Similarly, the two angles  $\Psi$  and  $\beta$  define the orientation of the aircraft  $x$  axis and velocity vector in Fig. 2.

The Euler and aerodynamic angles are used in stability and control analysis, while the flight path angles are used in point-mass trajectory analysis. It would benefit both analyses to visualize all three sets of angles at one time to analyze aircraft stability and maneuverability.

Another simplified model that is used to visualize aircraft maneuvers is shown in Fig. 4. It shows that if the aircraft rolls about the velocity vector (stability  $x$  axis for zero sideslip angle), the angle of attack is constant and the sideslip angle is constant (zero if the initial value is zero). This condition is true only if the direction of the velocity vector is constant, e.g., in a rotary balance wind tunnel test.

Rolling about the velocity vector is a good approximation of a coordinated maneuver for small roll oscillations about the wings' level steady-flight conditions. These conditions are normally used for lateral-directional stability analysis and control law design. For large-angle maneuvers, the balance between the lift and gravity vectors is disturbed and the direction of the velocity vector will change. In most cases, the reason for rolling is to change the direction of the velocity vector.

An example of a large-angle maneuver with a constant angle of attack (and sideslip angle) is a steady-level turn. In this case, the aircraft rotation vector is vertical in inertial space while the velocity vector is horizontal (the aircraft does not roll about the velocity vector). As will be shown later, for a more general coordinated maneuver with zero sideslip angle, the aircraft should roll about the axis of rotation of the velocity vector. In a steady-level turn, the velocity vector rotates about the inertial vertical axis in the same manner as the aircraft rotation vector.

To help visualize aircraft maneuvers, an alternative representation of aircraft angles called "spherical mapping" has been developed.<sup>2</sup> The angles involved and their interrelationships are clearly displayed on the same plot. The direction of the aircraft axis of rotation is readily shown, facilitating aircraft roll-axis control analysis. Spherical mapping is also used to derive important relationships among the aircraft angles defining the aircraft attitude, aerodynamic angles, and flight path angles.

### Spherical Mapping

The spherical mapping technique displays the aircraft angles on a two-dimensional surface of a unit sphere. We start the development of this technique by taking the two-dimensional plot of Fig. 1 and drawing a circle of unit radius

around the c.g., as shown in Fig. 5a. The angles between the vectors can be defined as arc length along the unit circle. The arc length can then be represented as a one-dimensional plot, as shown in Fig. 5b. The angles are represented as length along a line. This concept is extended to angles in three dimensions by representing the angles on a two-dimensional surface of a sphere of unit radius.

The angles are represented as arc length along great circles or dihedral angles between great circles, as shown in Figs. 6a and 6b. The aircraft heading angle  $\Psi$  and the flight path heading angle  $\sigma$  are measured from some reference heading direction, in a horizontal plane, along a great circle of the unit sphere. The aircraft pitch angle  $\theta$  is measured in a vertical plane containing the aircraft  $x$  axis, along a great circle. Similarly, the flight path elevation  $\gamma$  is measured in a vertical plane containing the velocity vector.

For the zero sideslip case (Fig. 6a), the velocity vector is in the  $x$ - $z$  plane of the aircraft (this is the definition of zero sideslip). The angle of attack  $\alpha$  is measured along the great circle containing the aircraft  $x$  axis and the velocity vector (in the aircraft  $x$ - $z$  plane). The aircraft roll angle  $\phi$  about the  $x$  axis is defined as the dihedral angle between the  $x$ - $z$  plane and the vertical plane through the aircraft  $x$  axis. If the  $x$ - $z$  plane is vertical, then the roll angle is zero, corresponding to the "wings level" condition.

The dihedral angle between the  $x$ - $z$  plane and the vertical plane through the velocity vector is defined as the bank angle  $\mu$ . For a small-value of angle of attack, the roll angle  $\phi$  and the bank angle  $\mu$  are approximately equal, where spherical triangles can be represented by linear triangles. The bank angle is the rotation of the  $x$ - $z$  plane about the velocity vector. Since the lift vector is perpendicular to the velocity vector and in the  $x$ - $z$  plane of the aircraft, the bank angle is the measure of lift-vector rotation. The bank angle is used in the point-mass trajectory calculations. The bank angle is zero when the  $x$ - $z$  plane is vertical.

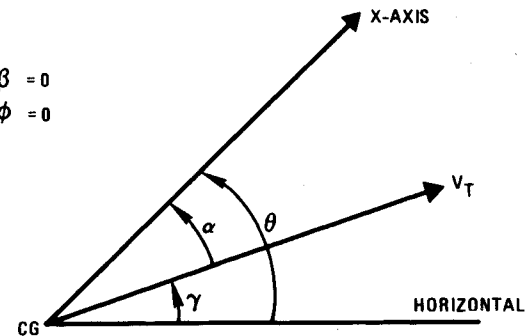


Fig. 1 Angular relationships for longitudinal motion with zero sideslip and roll angle.

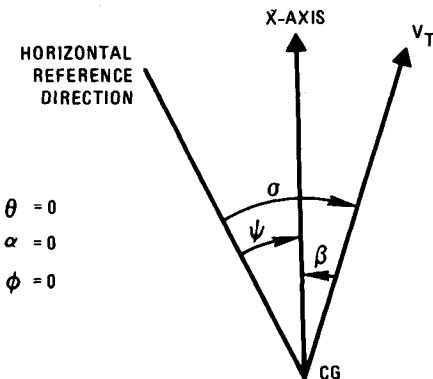


Fig. 2 Angular relationship for directional motion with zero pitch angle, angle of attack, and roll angle.

Fig. 3 Definition of Euler angles  $(\psi, \theta, \phi)$  and aerodynamic angles  $(\alpha, \beta)$ .

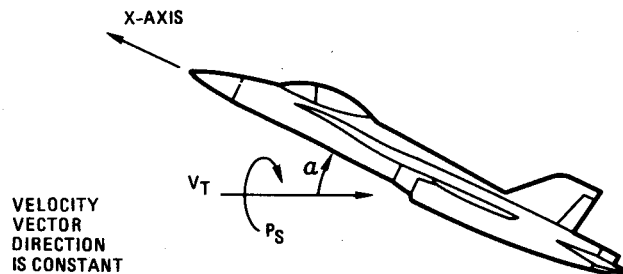
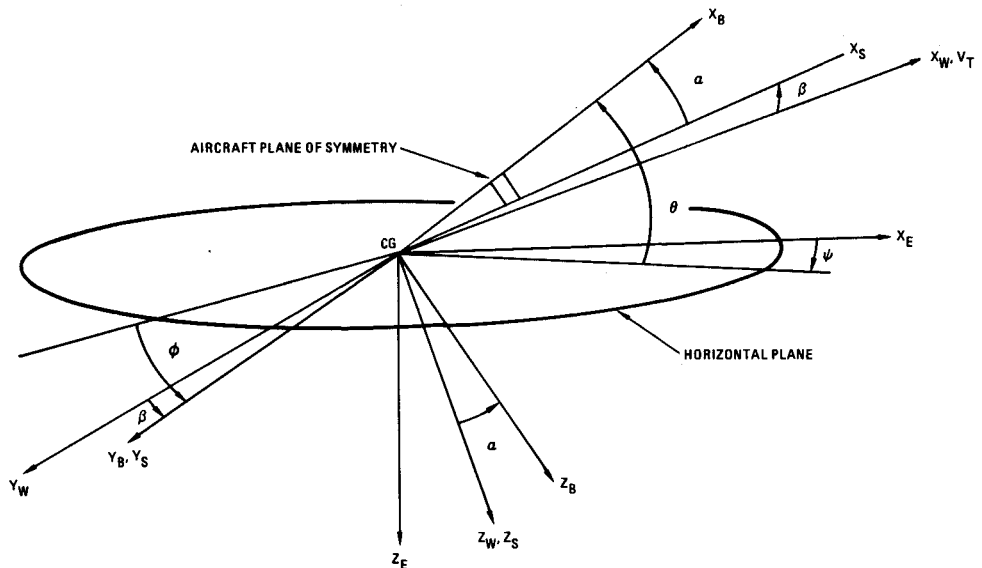


Fig. 4 Roll about velocity vector with constant angle of attack.

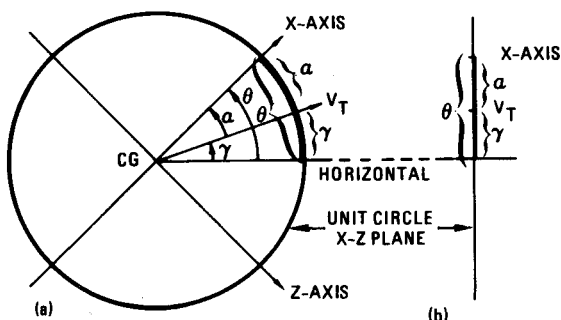


Fig. 5 Angles defined as arc length along unit circle.

For the nonzero sideslip angle case (Fig. 6b), the angle of attack is measured from the aircraft  $x$  axis to the projection of the velocity vector in the  $x$ - $z$  plane. The sideslip angle  $\beta$  is measured along the great circle containing the velocity vector and the projection of the velocity vector in the  $x$ - $z$  plane. The bank angle is the dihedral angle between the great circle defining sideslip and a plane perpendicular to the vertical plane at the velocity vector.

This two-dimensional plot (Fig. 6), on the surface of the unit sphere, shows the interrelationship between the Euler, aerodynamic, and flight path angles. It is more convenient to visualize the angles from the aircraft center of gravity, which is chosen as the center of the unit sphere as shown in Fig. 7a. For this "inside-out" representation, the positive heading angle is to the right and the positive roll angle is in clockwise rotation about the aircraft  $x$  axis. The linearized plot of the angular relationship is shown in Fig. 7b. This figure can be further simplified by only plotting the angle of attack and sideslip angle lines in an inertial azimuth and elevation coordinate

system, as shown in Fig. 7c. The aircraft azimuth and elevation are plotted at  $(\Psi, \theta)$  while the flight path azimuth and elevation is plotted at  $(\sigma, \gamma)$ . The azimuth and elevation of the velocity vector projection in the  $x$ - $z$  plane (stability  $x$  axis)  $(\sigma', \gamma')$  can be computed from the Euler angles and angle of attack with a sideslip angle equal to zero (see the next section). Connecting the three points with lines defines the  $\alpha$  and  $\beta$  lines. The roll angle  $\phi$  is the angle between the vertical and the  $\alpha$  line at the  $x$  axis. The bank angle  $\mu$  is the angle between the horizontal and the  $\beta$  line at the velocity vector. This plot (Fig. 7c) is used to display aircraft angles in maneuvering flight.

### Angular Relationships

The relationship among the three sets of angles can be computed by using spherical trigonometry. As an example, a portion of the spherical surface of Fig. 7a can be divided into spherical triangles, as shown in Fig. 8. This is only one example of many triangles that can be formed. By applying the laws of sine and of cosine to the spherical triangles, the angular relationships can be derived, as shown in Fig. 9. Each of the three sets of angles is a function of the other two sets.

### Simple Maneuvers

The change in the aircraft angle display due to the body axis rates  $(P, Q, R)$  is illustrated in Fig. 10. The aircraft is assumed to be initially at a nonzero roll angle with zero sideslip angle; the velocity vector is in the  $x$ - $z$  plane. The velocity vector direction is assumed to be constant for this example. A roll rate causes the  $x$ - $z$  plane to rotate about the  $x$  axis, which causes changes in the sideslip angle and angle of attack, as shown in Fig. 10a. A pitch rate causes the  $x$ - $z$  plane to rotate about the  $y$  axis, thereby increasing the angle of attack, as shown in Fig. 10b. A yaw rate causes the  $x$ - $z$  plane to rotate about the  $z$  axis, causing a change in the sideslip angle and a slight change in the angle of attack, as shown in Fig. 10c. Rotating the  $x$ - $z$  plane about the  $z$  axis causes the great circle to move approximately parallel near the  $x$  axis.

These simple motions can be combined to perform a maneuver to change the direction of the  $x$  axis from one point to another, as shown in Fig. 11. It requires only two rotations to change the elevation and azimuth of the aircraft, as shown in Figs. 11a and 11b. In both cases, the maneuver caused the sideslip angle to build up. If we put a zero sideslip angle constraint on the maneuver, then three rotations are required, as shown in Fig. 11c.

Combining a roll rate and yaw rate motion is equivalent to defining the rotation of the  $x$ - $z$  plane about an axis other

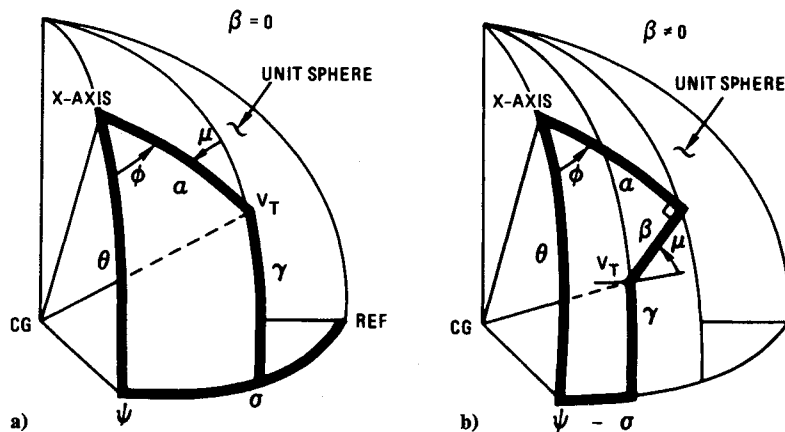


Fig. 6 Angles defined on a unit sphere.

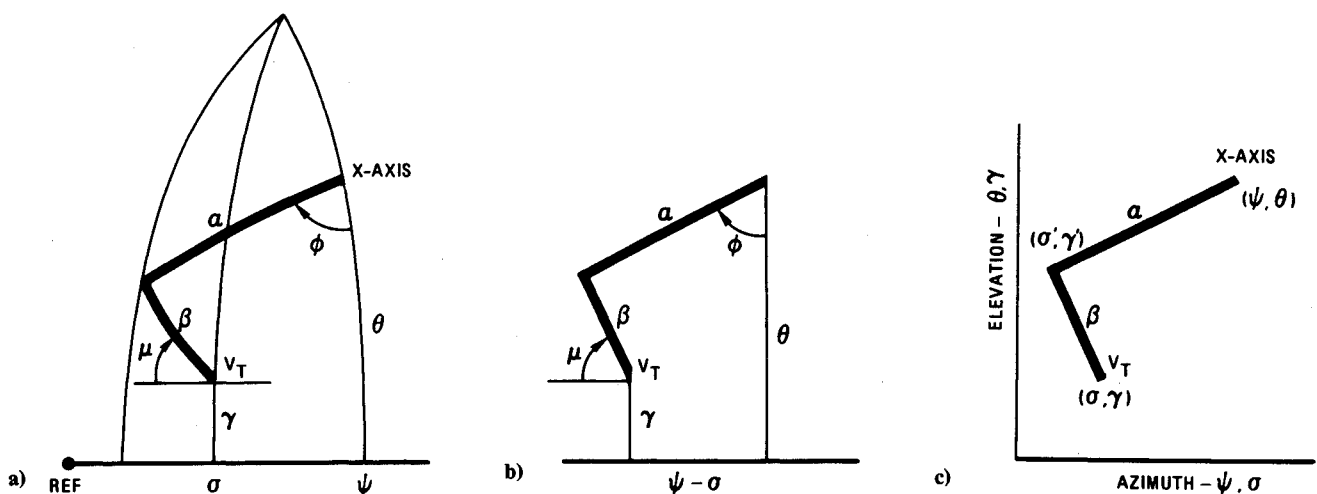


Fig. 7 a) Inside-out view from center of sphere, b) linearized plot, and c) plotted in elevation and azimuth coordinates.

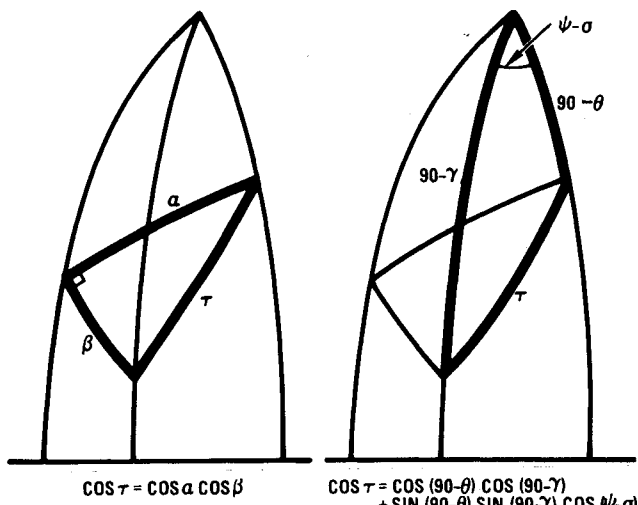


Fig. 8 Spherical trigonometry is used to derive angular relationships.

than the  $x$  and  $z$  axes. In the example of Fig. 11c, the rotation is about the velocity vector  $V_T$ .

The term "roll axis of the aircraft" has two meanings. In flight dynamic analysis, we take the total rotation vector of the aircraft  $\omega$  and resolve it into components along three body axes. The component along the  $x$  axis is roll rate  $P$ , along the  $y$  axis pitch rate  $Q$ , and along the  $z$  axis yaw rate  $R$ . Therefore, the  $x$  axis is defined as the roll axis.

In maneuvering flight, a coordinated maneuver is defined in terms of pitching and rolling the aircraft. The pitching maneuver is the rotation of the  $x$ - $z$  plane about the aircraft  $y$  axis. The rolling maneuver is the rotation of the  $x$ - $z$  plane about an axis to keep sideslip small. For small-angle rolling motion, where the velocity vector does not change direction, a coordinated maneuver is achieved by rolling about the velocity vector, as depicted in Fig. 11c. In large-angle maneuvering flight, roll axis control means controlling the axis about which the aircraft  $x$ - $z$  plane rotates. This is the second definition of "aircraft roll axis." This definition will be used throughout the balance of this paper.

For large-angle roll maneuvers, the velocity vector direction changes due to a change in the direction of the forces on the aircraft. In this case, rolling the aircraft about the velocity vector does not achieve a coordinated zero-sideslip angle maneuver, since the velocity vector changes direction. A coordinated maneuver is achieved by rolling the aircraft about the axis of rotation of the velocity vector, as shown in Fig. 12. The direction of the aircraft axis of rotation and the velocity vector's axis of rotation can be computed from measured parameters.

### Axes of Rotation

The direction of the aircraft's axis of rotation in body coordinates can be defined by two angles  $(\alpha_R, \beta_R)$ , similarly to the way we define the direction of the velocity vector by  $(\alpha, \beta)$  as shown in Fig. 13a for  $\alpha_R$ . This diagram is drawn for a positive roll and yaw rate where the vectors are along the positive  $x$  and  $z$  axes. For a negative roll rate, the vector would be along the negative  $x$  axis and  $\alpha_R$  would be greater than 90 deg (solid line in Fig. 13b).

FLIGHT PATH ANGLES,  $(\gamma, \alpha, \mu) = f(\alpha, \beta, \theta, \psi, \phi)$ 

$$\sin \gamma = (\cos \alpha \sin \theta - \sin \alpha \cos \theta \cos \phi) \cos \beta + (-\cos \theta \sin \phi) \sin \beta$$

$$\begin{aligned} \sin(\theta - \psi) \cos \gamma &= (-\sin \alpha \sin \phi) \cos \beta + (\cos \phi) \sin \beta \\ \cos(\theta - \psi) \cos \gamma &= (\cos \alpha \cos \theta + \sin \alpha \sin \theta \cos \phi) \cos \beta + (\sin \theta \sin \phi) \sin \beta \end{aligned}$$

$$\begin{aligned} \sin \mu \cos \gamma &= (\cos \theta \sin \phi) \cos \beta + (\cos \alpha \sin \theta - \sin \alpha \cos \theta \cos \phi) \sin \beta \\ \cos \mu \cos \gamma &= (\cos \alpha \cos \theta \cos \phi + \sin \alpha \sin \theta) \end{aligned}$$

EULER ANGLES,  $(\theta, \psi, \phi) = f(\alpha, \beta, \gamma, \sigma, \mu)$ 

$$\sin \theta = (\sin \alpha \cos \gamma \cos \mu) + (\cos \alpha \sin \gamma) \cos \beta + (\cos \alpha \cos \gamma \sin \mu) \sin \beta$$

$$\begin{aligned} \sin(\psi - \phi) \cos \theta &= (\sin \alpha \sin \mu) + (-\cos \alpha \cos \mu) \sin \beta \\ \cos(\psi - \phi) \cos \theta &= (-\sin \alpha \sin \gamma \cos \mu) + (\cos \alpha \cos \gamma) \cos \beta + (-\cos \alpha \sin \gamma \sin \mu) \sin \beta \end{aligned}$$

$$\begin{aligned} \sin \phi \cos \theta &= (\cos \gamma \sin \mu) \cos \beta + (-\sin \gamma) \sin \beta \\ \cos \phi \cos \theta &= (\cos \alpha \cos \gamma \cos \mu) + (-\sin \alpha \sin \gamma) \cos \beta + (-\sin \alpha \cos \gamma \sin \mu) \sin \beta \end{aligned}$$

AERODYNAMIC ANGLES,  $(\alpha, \beta) = f(\theta, \psi, \phi, \gamma, \sigma)$ 

$$\sin \beta = \cos \gamma [\sin \theta \sin \phi \cos(\theta - \psi) + \cos \phi \sin(\theta - \psi)] - \sin \gamma [\cos \theta \sin \phi]$$

$$\sin \alpha \cos \beta = \cos \gamma [\sin \theta \cos \phi \cos(\theta - \psi) - \sin \phi \sin(\theta - \psi)] - \sin \gamma [\cos \theta \cos \phi]$$

$$\cos \alpha \cos \beta = \cos \gamma [\cos \theta \cos(\theta - \psi)] + \sin \gamma [\sin \theta]$$

Fig. 9 Relationships among Euler angles, flight path angles, and aerodynamic angles.

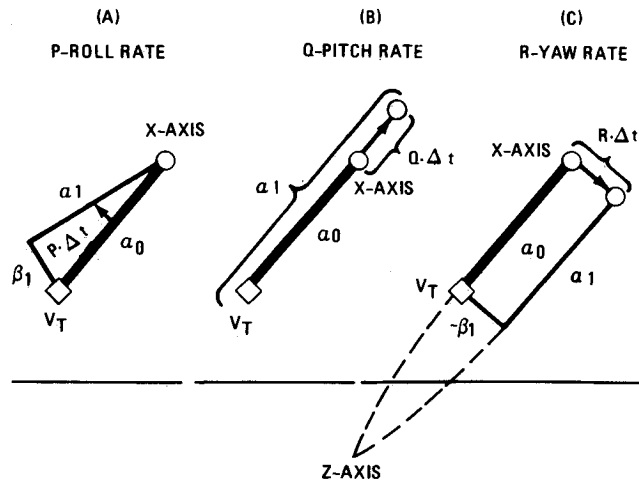


Fig. 10 Aircraft attitude change due to body axis rotations.

To be able to relate more conveniently the rotation axis to the velocity vector for both positive and negative roll rate, the rotation vector is reflected to the forward hemisphere, as shown in Fig. 13b (broken line). The  $\beta_R$  due to the pitch rate is defined similarly to the aerodynamic angle  $\beta$ . The equations for the rotation vector angles are:

$$\omega_{PR} = \text{sign}(P) \sqrt{P^2 + R^2} \quad (1)$$

$$\sin \alpha_R = \frac{R}{\omega_{PR}}, \quad \cos \alpha_R = \frac{P}{\omega_{PR}} \quad (2)$$

$$\omega = \text{sign}(P) \sqrt{\omega_{PR}^2 + Q^2} \quad (3)$$

$$\sin \beta_R = \frac{Q}{\omega}, \quad \cos \beta_R = \frac{\omega_{PR}}{\omega} \quad (4)$$

The rate of change of the velocity vector direction is a function of the aircraft total load factor, the direction of the gravity vector, and the total velocity. To compute these angles, we can start with the equations for the rate of change

VELOCITY VECTOR DIRECTION IS CONSTANT

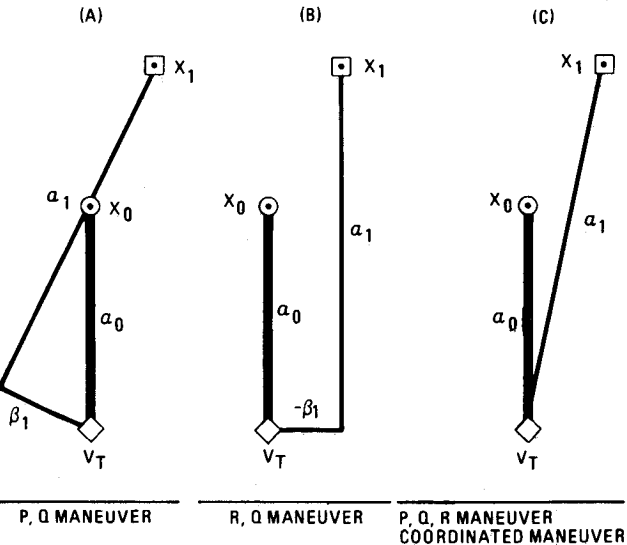
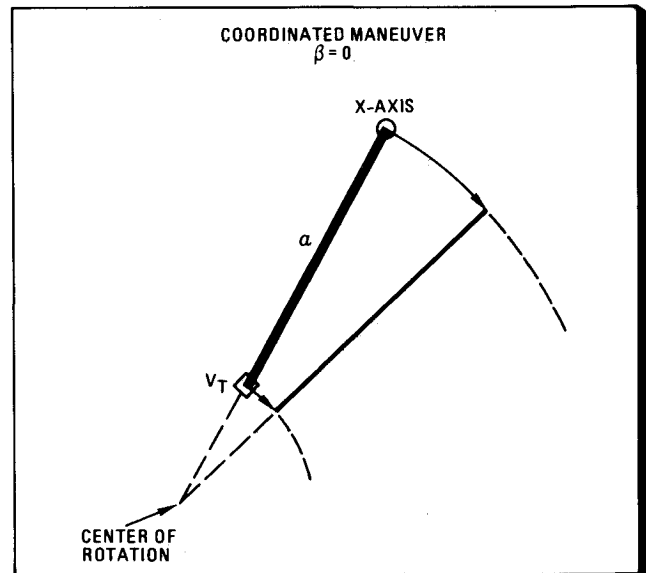
Fig. 11 Representation of aircraft maneuvering from  $\circ$  to  $\square$ .

Fig. 12 For a coordinated maneuver, the aircraft rolls about velocity vector axis of rotation.

of the flight path angles:

$$\begin{aligned} \dot{\sigma} &= \frac{g}{V_T \cos \gamma} [n_x (\sin \alpha \sin \mu - \cos \alpha \sin \beta \cos \mu) \\ &\quad + n_y (\cos \beta \cos \mu) + n_z (\cos \alpha \sin \mu + \sin \alpha \sin \beta \cos \mu)] \quad (5) \end{aligned}$$

$$\begin{aligned} \dot{\gamma} &= \frac{g}{V_T} [n_x (\sin \alpha \cos \mu + \cos \alpha \sin \beta \sin \mu) - n_y (\cos \beta \sin \mu) \\ &\quad + n_z (\cos \alpha \cos \mu - \sin \alpha \sin \beta \sin \mu) - \cos \gamma] \quad (6) \end{aligned}$$

$$\begin{aligned} \dot{\mu} &= (P \cos \alpha + R \sin \alpha) \sec \beta + \dot{\sigma} \sin \gamma \\ &\quad + \frac{g}{V_T} (n_x \sin \alpha + n_z \cos \alpha - \cos \mu \cos \gamma) \tan \beta \quad (7) \end{aligned}$$

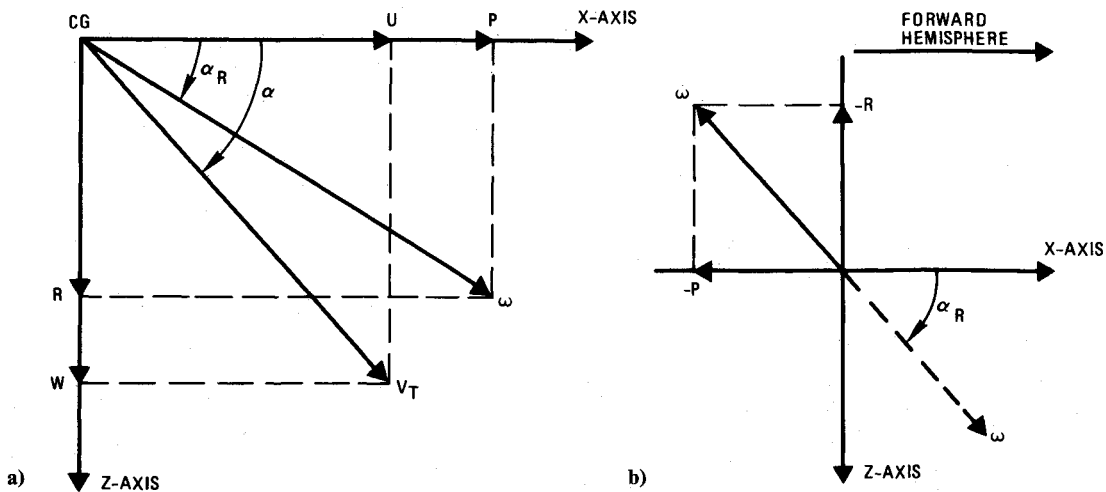


Fig. 13 a) Direction of rotation vector is defined similarly to direction of velocity vector; b) rotation vector is reflected to the forward hemisphere.

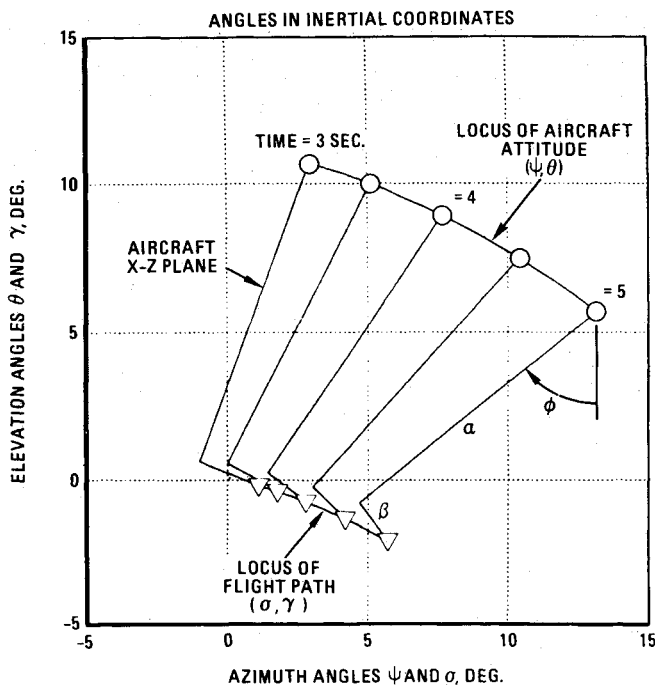


Fig. 14 Graphical display of dynamic maneuver.

These flight path angular rates are transformed to the wind axis orthogonal body coordinate system by using the inverse Euler angular rate transformation:

$$P_{vw} = \dot{\mu} - \dot{\sigma} \sin \gamma \quad (8)$$

$$Q_{vw} = \dot{\gamma} \cos \mu + \dot{\sigma} \sin \mu \cos \gamma \quad (9)$$

$$R_{vw} = \dot{\sigma} \cos \mu \cos \gamma - \dot{\gamma} \sin \mu \quad (10)$$

The flight path angular rates are then transformed from wind axes to body axes through an angle of attack and sideslip angle transformation:

$$P_v = P_{vw} \cos \alpha \cos \beta - Q_{vw} \cos \alpha \sin \beta - R_{vw} \sin \alpha \quad (11)$$

$$Q_v = P_{vw} \sin \beta + Q_{vw} \cos \beta \quad (12)$$

$$R_v = P_{vw} \sin \alpha \cos \beta - Q_{vw} \sin \alpha \sin \beta + R_{vw} \cos \alpha \quad (13)$$

The three rate components ( $P_v, Q_v, R_v$ ) are the velocity vector rotational rate components in body coordinates. These rate components can be used to define the axis of rotation of the velocity vector in body coordinates ( $\alpha_v, \beta_v$ ) by using the same equations previously given to define  $\alpha_R$  and  $\beta_R$ .

One practical consideration in the computation of the rotational axis direction is that if the rotational rate is zero (for either the aircraft or the velocity vector), then there is no axis of rotation. In this case  $\alpha_R$  and  $\beta_R$  can be set to zero for no aircraft rotation and  $\alpha_v$  and  $\beta_v$  can be set to  $\alpha$  and  $\beta$  if there is no velocity vector rotation. The directions of the rotation axes are defined in inertial coordinates ( $\sigma_R, \gamma_R$ ) and ( $\sigma_v, \gamma_v$ ) by using the equations of Fig. 9.

### Display of Maneuvers

The main advantage of the spherical mapping representation of the aircraft angles is that it facilitates the display of dynamic maneuvers. To illustrate this, a portion of an aircraft rolling maneuver is depicted in Fig. 14. This is an uncoordinated maneuver since the sideslip angle is nonzero. The figure shows the locus of the aircraft attitude angles ( $\psi, \theta$ ) and the flight path angles ( $\sigma, \gamma$ ). The line segments connecting the aircraft  $x$  axis and the flight path represent the angle of attack and sideslip at the indicated unit of time. The roll angle  $\phi$  is represented as an angle between the aircraft  $x$ - $z$  plane ( $\alpha$  line) and the vertical. The figure shows that sideslip is decreasing during the illustrated portion of the maneuver. The complete roll maneuver is shown in Fig. 15. The aircraft and velocity vector axes of rotation are also shown.

The maneuver starts from the wing level ( $x$ - $z$  plane vertical), in level flight ( $\gamma = 0$ ), and with the angle of attack and pitch angle equal to approximately 11 deg. The aircraft has rolled to about 90 deg after 7 s. The maximum sideslip angle of approximately 2 deg occurs at 6.5 s. At 10 s, the aircraft has rolled to approximately 160 deg, the sideslip angle is close to zero, and the angle of attack has reduced to approximately 4 deg.

At 9 s, the aircraft  $x$ - $z$  plane line is extended to show the  $\alpha$  and  $\beta$  of the two rotation vectors. The projection of the aircraft and velocity vector rotation vectors in the  $x$ - $z$  plane,  $\alpha_R$  and  $\alpha_v$ , are not equal; therefore, the maneuver is not a constant sideslip maneuver. The flight path pitch rate  $Q_v$  is greater than the aircraft pitch rate  $Q_R$  ( $\beta_v > \beta_R$ ); therefore, the angle of attack is decreasing.

A similar roll maneuver, but one with a computed rudder input to coordinate the maneuver (zero sideslip angle), is

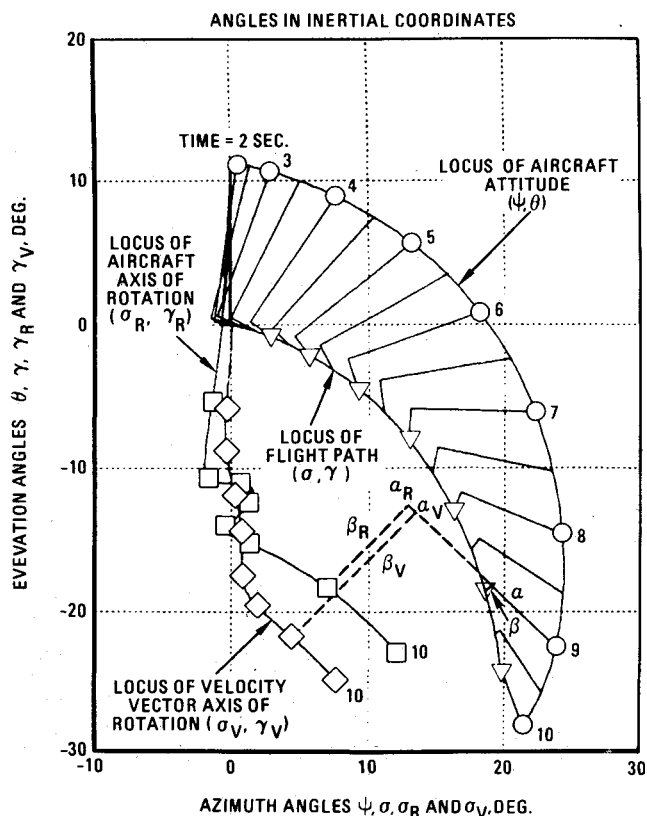


Fig. 15 Display of aircraft and flight path attitude and axes of rotation for roll maneuver.

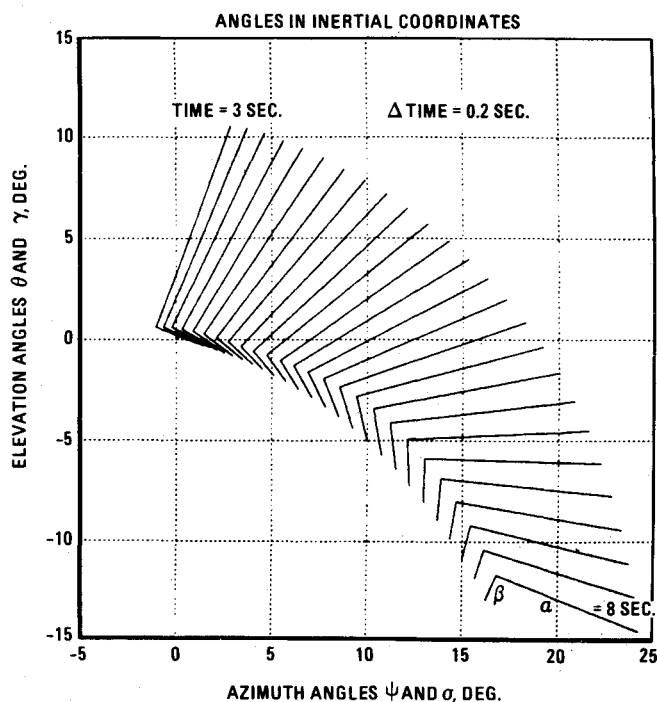


Fig. 17 Display of aircraft alpha and beta lines.

shown in Fig. 16. It can be observed that, for the coordinated maneuver, the aircraft does not roll about the velocity vector. At the initiation of the maneuver, both the aircraft and velocity vector rotation axes are along the velocity vector. As the velocity vector changes direction, the two axes of rotation are not along the velocity vector.

Spherical mapping can be used to display aircraft maneuvers in real-time simulations or from flight tests. For real-time maneuvers, it is best to display only the angle of attack and sideslip angle lines, as shown in Fig. 17. The number of displayed lines should be limited to approximately 10 lines for 2 s of flight to keep the display clear. As a new pair of angle of attack and sideslip angle lines is added, the first displayed pair of lines is faded out. The change of position and attitude of the new lines, being displayed at a fixed rate, gives an indication of the aircraft maneuvering rate.

Other information that can be displayed by the spherical mapping technique are the pipper position and target direction in air-to-air combat maneuvering. The pipper position in body coordinates can be defined by two angles ( $\alpha_p, \beta_p$ ) and transformed to inertial coordinates ( $\sigma_p, \gamma_p$ ) by using the equations of Fig. 9. The inertial direction of the target relative to the aircraft can be computed from the relative target position ( $X_T, Y_T, H_T$ ) and the aircraft position ( $X_A, Y_A, H_A$ ) coordinates:

$$\Delta X = X_T - X_A \quad \Delta Y = Y_T - Y_A \quad (14)$$

$$\Delta H = H_T - H_A \quad (15)$$

$$\Delta' = \sqrt{\Delta X^2 + \Delta Y^2} \quad \Delta = \sqrt{\Delta X^2 + \Delta Y^2 + \Delta H^2} \quad (16)$$

$$\sin \sigma_T = \frac{\Delta Y}{\Delta'} \quad \cos \sigma_T = \frac{\Delta X}{\Delta'} \quad (17)$$

$$\sin \gamma_T = \frac{\Delta H}{\Delta} \quad \cos \gamma_T = \frac{\Delta'}{\Delta} \quad (18)$$

The display of pipper and target positions, together with aircraft attitude in maneuvering flight, is useful in visualizing air-to-air combat maneuvering techniques.

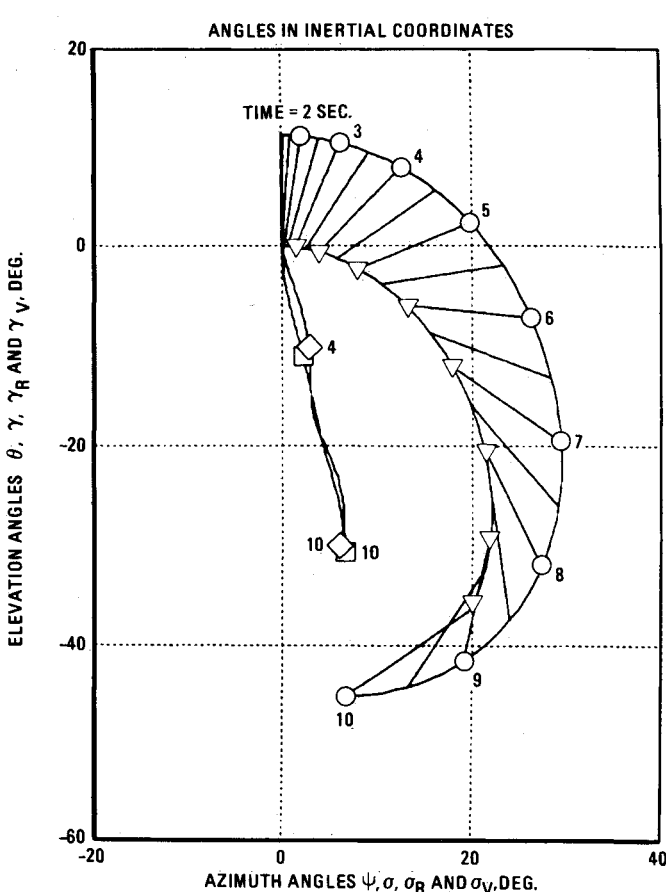


Fig. 16 A zero sideslip angle coordinated roll maneuver.

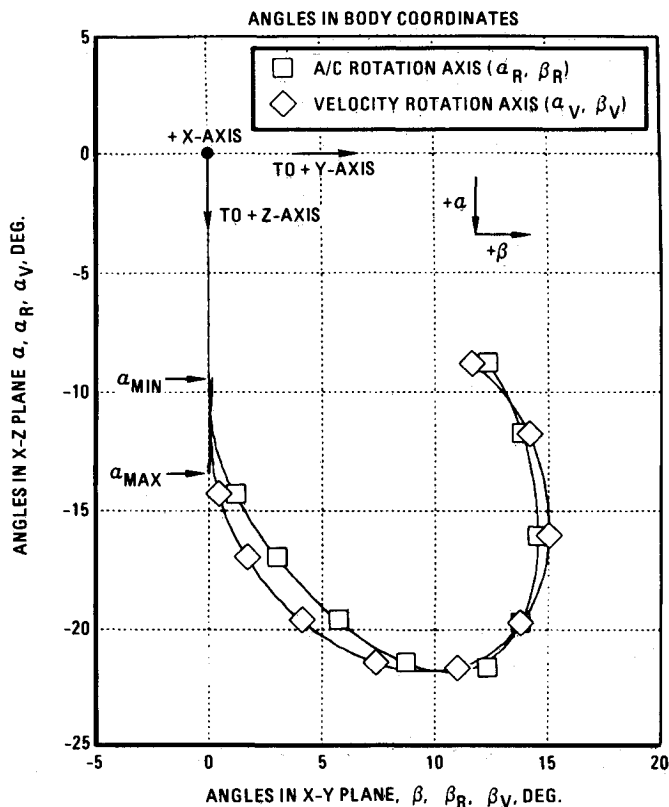


Fig. 18 Display of velocity vector and rotation axes in body coordinates.

Another way to visualize aircraft maneuvering flight is to display the angles in body coordinates. This would be equivalent to the standard head-up-display format. As an example, a portion of the coordinated maneuver of Fig. 16 is shown in Fig. 18. The (0,0) value represents the aircraft  $x$  axis. The aircraft positive  $z$  axis is 90 deg below the  $x$  axis, while the aircraft positive  $y$  axis is 90 deg to the right of the  $x$  axis. The positive value of the angle of attack is defined in the vertical downward direction, while the positive sideslip angle is defined in the horizontal right direction.

Figure 18 shows the locus of the velocity vector and the directions of the two rotation axes. For this coordinated maneuver, the sideslip angle is zero and the velocity vector locus is in the  $x$ - $z$  plane. The projection of the rotation axis directions in the  $x$ - $z$  plane ( $\alpha_R$  and  $\alpha_V$ ) are equal. This means that the aircraft and the velocity vector rotate about the same axis in the  $x$ - $z$  plane, and that is the reason that the sideslip angle is constant (zero).

The sideslip angles of the rotation axes ( $\beta_R$  and  $\beta_V$ ) are proportional to the aircraft and velocity vector rotation components in the aircraft  $x$ - $z$  plane. For the maneuver displayed in Fig. 18,  $\beta_R$  is greater than  $\beta_V$ . This means that the aircraft pitch rate is greater than the velocity vector pitch rate; therefore, the angle of attack is increasing. For a maneuver with a constant angle of attack and sideslip angle, the two rotation axes would be superimposed.

The body axis plot can also be used to display the target and pipper positions in addition to the rotation axes and the velocity vector to analyze aircraft tracking maneuvers. The body axis angle of the target ( $\alpha_T, \beta_T$ ) can be computed from the inertial target angles ( $\sigma_T, \gamma_T$ ) by using the equations of Fig. 9.

### Concluding Remarks

The spherical mapping technique that has been developed is useful for the visualization of angular relationships in maneuvering flight. Conceptually, the angles are displayed on the surface of a unit sphere. In practice, the spherical surface has been linearized in terms of an orthogonal plot of azimuth and elevation angles. For large elevation angles, the linearization causes a distortion of the displayed  $\alpha$ ,  $\beta$ ,  $\phi$ , and  $\mu$  angles. The distortion can be reduced by several means: 1) computing the azimuth and elevation of points along the  $\alpha$  and  $\beta$  lines (approximately every 2 deg) causes these great circle lines to become curved, reducing the distortion of the displayed  $\phi$  and  $\mu$  angles, and 2) reducing the spacing of the constant azimuth lines as a function of the elevation angle reduces the distortion of the  $\alpha$  and  $\beta$  line length. Other "mapping" techniques can be used to display the surface of the sphere on a linear plot.

The main advantage of the spherical mapping display is that it allows one to interpret three-dimensional angular relationships in two dimensions. One can simply take a set of angles from flight test or simulation results and sketch the angular relationships.

### Acknowledgments

This work was performed under the Independent Research and Development Program at Northrop. The author wishes to acknowledge Lloyd Stout for his work on the computer graphics display and the development of the velocity vector rotation axis equations.

### References

- 1 Mitchell, D. G., Myers, T. T., Teper, G. L., and Johnston, D. E., "Investigation of High-Angle-of-Attack Maneuver-Limiting Factors," AFWAL-TR-80-3141, Dec. 1980.
- 2 Kalviste, J., "Representation and Analysis of Airplane Angles by Spherical Mapping," Northrop Corp., Hawthorne, CA, Rept. NOR-75-144, Oct. 1975.